BioNanoScience
https://doi.org/10.1007/s12668-024-01572-0

RESEARCH

Preparation of NiO Nanosheets in a Lyotropic Liquid Crystal Medium and Their Application in Catalytic, Anti-Cancer and Anti-Bacterial Activities

PR. Meyyathal[1,2] · N. Santhiya[1] · R. Dharani[1] · S. Umadevi[1]

Accepted: 24 July 2024

Abstract
Herein, we report the preparation of nickel oxide (NiO) nanosheets in a lyotropic liquid crystal (LLC) medium via a chemical reduction method. The LLC phase exhibiting a lamellar phase was formed using a binary mixture of triton X-100 (68 wt%) and water (32 wt%) at 4 °C. The nanomaterials were prepared in this medium by reducing $NiCl_2.6H_2O$ using a strong reducing agent, $NaBH_4$. The prepared nanomaterials were characterized through UV–Vis, SEM, FT-IR and XPS techniques. The NiO nanomaterials were found to exhibit good catalytic activity towards reduction and degradation reactions. An apparent rate constant (K_{app}) value of 1.4×10^{-2} min^{-1} was obtained for the reduction reaction of 4-nitrophenol to 4-aminophenol using NiO nanomaterials (300 µL of as-prepared 80 mM dispersion). The nanomaterials showed good recyclability with effective activity until 5th cycle. Further, K_{app} of 0.5×10^{-2} min^{-1} was obtained for the degradation reaction of methylene blue. The anti-bacterial studies suggested that the NiO nanomaterials were effective against gram positive (*S. aureus*) bacteria and anti-cancer studies of the particles against breast cancer cells (MCF-7) showed an IC_{50} value of 78.93 µg/mL.

Keywords Lyotropic liquid crystal · Lamellar · Catalytic · Anti-cancer · Anti-bacterial

1 Introduction

Liquid crystal (LC) is an intermediate state that possesses the properties between liquid (isotropic) and solid (anisotropic). The LCs are categorized into thermotropic and lyotropic liquid crystals (LLCs), based on their physical as well as chemical properties [1]. The LLC medium is composed of amphiphilic molecules in a suitable solvent. The supramolecular arrangement in a LLC phase can be tuned (such as lamellar, cubic, hexagonal etc.) by varying the concentration of amphiphilic molecules in the solvent and temperature [2]. Using LLCs with different phase structures, nanoparticles (NPs) with different morphologies, controlled growth, desired size and shape can be achieved. The nucleation and growth were affected because of the long-range order of LLCs, which leads to the different morphology of the NPs [3, 4]. The LLCs assisted synthesis of NPs benefits from the advantages that the synthesised NPs are stable and aggregation-free in the LLC medium without the help of a stabilizing agent.

Few examples of preparation of nanoparticles in a LLC medium are provided below.

Qi et al. [5] prepared the ribbon-like silver (Ag) NPs using lamellar LLC as a reaction medium and tetraethylene glycol monododecyl ether ($C_{12}E_4$) as a non-ionic surfactant as well as a reductant. Patakfalvi et al. [6] prepared the Ag NPs and explained the stability of the Ag NPs with respect to the lamellar distance. i.e., the prepared NPs were highly stable with a larger lamellar distance than the NPs with a smaller lamellar distance. Our most recent publications [7–9] describe the synthesis of gold (Au), Ag and copper (Cu) nano- and microparticles (MPs) in a hexagonal and lamellar LLC medium. While nearly spherical Au NPs formed in a lamellar mesophase, star-shaped anisotropic particles were obtained in a hexagonal medium [7]. Anisotropic Ag MPs were formed in a hexagonal LLC medium, and the particles remained stable for several months without aggregating [8]. Cu MPs with good catalytic activity were

✉ S. Umadevi
umadevilc@gmail.com; umadevis@alagappauniversity.ac.in

[1] Department of Industrial Chemistry, Alagappa University, Karaikudi 630003, Tamil Nadu, India

[2] District Institute of Education and Training (DIET), Sivagangai, Kalaiyarkoil 630551, Tamil Nadu, India

Published online: 08 August 2024

prepared in a hexagonal LLC medium [9]. Anisotropic gold nanostars (short—spiked as well as long—spiked) prepared in a hexagonal LLC medium were explored for sensing applications based on surface-enhanced Raman scattering [10].

In recent years, nickel oxide (NiO) nanomaterials have attracted significant interest owing to their potential applications in various fields such as batteries, supercapacitors, optical amplifiers, tuneable lasers, catalysis, dye degradation, biomedicine, etc. [11]. The NiO nanomaterials were prepared using various methods. For instance, Dharmaraj et al. synthesised the NiO NPs having a cubic shape by a chemical method in which nickel acetate and poly (vinyl acetate) were used as the precursors at 723 K [12]. Niasari et al. [13] prepared the nickel (Ni) as well as NiO NPs by a thermal process (400–900 °C) without the use of surfactants or solvents, using nickel octanoate as a precursor. It was a simple precipitation method and the prepared NiO NPs showed spherical morphology. The synthesis of NiO NPs was also achieved using eco-friendly techniques. For example, the laser source was used for the preparation of NiO NPs, in which Ni metal was soaked in 3% H_2O_2. The usage of chemicals as well as starting materials was reduced in this process. As a result, granular-shaped NPs were obtained [14]. Danial et al. [15] described the preparation of NiO NPs using the sol–gel method. In this study, a change in the morphology of the NPs was observed during the annealing process; the NiO NPs prepared at 200 °C were of smaller size whereas the particles prepared at 600 °C were found to be larger in size. A greener approach was carried out by Sabouri et al. [16] for the synthesis of NiO NPs using the sol–gel method, in which nickel nitrate, egg white and nickel were used to synthesise the controlled, regular-shaped NiO NPs. The synthesised NiO NPs were found to degrade the methylene blue (MB) by about 70% in presence of UV-A light. Also, while conducting a cytotoxicity test (MTT) on U87MG cell lines, NPs at a concentration (IC_{50}) of 15.62 µg/mL killed 50% of the cells [16]. The use of biomass such as plant petals and leaves having porous structures was also explored for the synthesis of Ni and NiO NPs to achieve a controlled size and prevent agglomeration [17]. For instance, utilising the *Okra* plant extract as a reducing and limiting agent, NiO NPs were synthesised through the sol–gel method [18]. The NiO NPs demonstrated a super-paramagnetic behaviour during magnetic experiments. The NiO NPs were also tested for cell cytotoxicity on multiple tumour cells by the MTT technique, antibacterial activity against gram-positive, gram-negative bacteria and photocatalytic activity against MB. The NiO NPs effectively decreased the percentage of cell viability and showed excellent photocatalytic activity through the complete degradation of MB under UV light. According to an antibacterial investigation, NiO NPs activity for gram-positive bacteria species is significantly more evident than that for gram-negative bacteria species [19]. Sabouri et al. [19] have also synthesised the evenly distributed, spherical-shaped NiO NPs using the same method mentioned above. In this study, the authors have used the *Salvia macrosiphon* boiss plant extract as a limiting agent. The synthesised NiO NPs showed decreased cell viability when the particles were tested on the Neuro2A cell lines and also showed 80% degradation of MB under UV-A light (11 W). Moreover, Sabouri et al. [20] have also synthesised the NiO nanosheets, utilising *Tragacanth* as a stabilising agent and nickel nitrate as a reducing agent through the co-precipitation method. The nanosheets had a cubic structure, Fm3m space group and a size of 18–43 nm, as examined by the XRD technique. The photocatalytic activity of the nanosheets was tested on dyes such as MB and methyl orange (MO) and obtained a degradation percentage of 79% (in 300 min) and 82% (in 210 min), respectively. The NiO NPs having the face-centred cubic structure and the space group Fm3m have been synthesised through the sol–gel method using *Cydonia oblonga* extract [21]. Ghazal et al. [21] reported that the NiO NPs had a band gap of 4.3 to 5.2 eV and effectively degraded the Rhodamine B dye under UV-A light. Furthermore, the non-cytotoxic effects of NiO NPs were demonstrated by the MTT test findings on L929 cell lines. Further, the NiO NPs having a spherical shape and size of ~ 59 nm were synthesised by Sabouri et al. [22] using the sol–gel method, in which a biopolymer, namely, *Arabic* gum, acted as a stabilising agent. The NiO NPs were tested for their antibacterial activity against the gram-positive (*Staphylococcus aureus, Bacillus subtilis*) as well as the gram-negative bacteria (*Escherichia coli, Pseudomonas aeruginosa*) and the results showed that, with the exception of *Bacillus subtilis* bacteria, which did not grow at a concentration of 10 mM, all bacterial resistance was ascribed to NiO NPs. Further, Strong cytotoxicity against U87MG cancer cells was demonstrated by the synthesised NPs (IC_{50}: 37.84 µg mL^{-1}), which also achieved 80% of MB degradation upon UV-A irradiation. Another example of the synthesis of spherical-shaped NiO NPs (particle size ~ 30 nm) using a greener approach was done by Sabouri et al. [23]. In this study, NiO NPs synthesis were carried out through the sol–gel method, in which *Salvia hispanica* L. (Chia) was used as a capping agent. As a result, the NiO NPs degraded 83% of the MB dye within 150 min upon UV-A (11 W) light. In addition to a concentration-dependent behaviour, the cytotoxicity results of the experiment conducted on the PC12 cell line showed dose-associated toxicity. Prabhu et al. [24] described the synthesis of NiO NPs using *Clitoria ternatea* flower extract as a precursor. The synthesised NiO NPs were used for the photocatalytic degradation of dyes such as Fast Green (FG) and Rose Bengal (RB) in the presence of sunlight and degradation percentages of 88.8% (FG) and 76.64% (RB) were achieved by NiO NPs. Further, NiO

NPs were tested for their anti-bacterial activity and found to be active against the gram-negative *E. coli* bacteria. The NiO NPs were most widely used in a variety of applications, such as energy storage, catalytic activity and biomedical applications such as anti-fungal and anti-bacterial activities [11]. Ali et al. [25] prepared the NiO NPs from *Lactuca serriola* seeds and the authors studied the anti-bacterial and photocatalytic activities of the obtained NPs. Sahila et al. [26] proposed the green synthesis of NiO NPs using *Allium cepa* (onion) bulb extract and the prepared NiO NPs were analysed for their dielectric properties at various concentrations. Abbaszadeh et al. [27] have reported the preparation of NiO NPs and their anticancer activity against the MCF-7 breast cancer cell lines. The method of preparation had the greatest impact on the effectiveness and morphology of the resulting NPs [15].

In this present study, NiO nanomaterials were prepared in the lamellar LLC medium (water and TX-100 in the ratio 3.2: 6.8) using $NaBH_4$ as the reducing agent without any external stabilizing agent. TEM images showed that the prepared NiO nanomaterials formed an agglomerated, tangled thread-like network. The prepared nanomaterials were effective against the MCF-7 breast cancer cell line with an IC_{50} value of 78.93 µg/mL. The nanomaterials showed better anti-bacterial activity against gram-positive bacteria. The catalytic activity of the NiO nanomaterials was tested against 4-nitrophenol and MB. The NiO nanomaterials showed better reduction and degradation properties.

2 Experimental

2.1 Materials and Methods

Nickel (II) chloride hexahydrate ($NiCl_2.6H_2O$), 4-nitrophenol and triton X-100 (TX-100) were obtained from Sigma Aldrich. $NaBH_4$ and MB were obtained from Merck Ltd.

UV–Vis studies were carried out using a Shimadzu UV-2401 PC (Shimadzu Corporation, Japan) spectrophotometer by employing a quartz cell of 1 cm path length. The Surface morphology of the nanomaterials was studied using EVO18 (CARL ZEISS, Germany) scanning electron microscopy (SEM) and the transmission electron microscopy (TEM) (Model: JEOL-2100 + , Country: Germany). Further, the presence of functional groups was confirmed using a Bruker Tenser 27 Fourier transform infrared (FT-IR) spectrometer (Bruker Optic GmbH, Germany) using KBr pellets. X-ray photoelectron spectroscopy (XPS ESCALab250, Thermo Scientific, USA) was used for elemental analysis.

2.2 Preparation of NiO Nanomaterials in a Lamellar LLC Template

NiO nanomaterials were prepared in the lamellar LLC medium by dissolving $NiCl_2.6H_2O$ (0.2 g, 0.8 mmol) in 3.2 mL of water and 6.8 mL of TX-100 (0.8:1.7 wt%). The temperature of the solution was maintained at 4 °C. To this solution, $NaBH_4$ (0.1 g, 2.6 mM) was slowly added and mixed well; colour of the solution changed from green to black within 1–2 min (Scheme 1). When the hydrogen gas release stopped, a black colour precipitate was obtained, which was washed with deionized water several times to remove excess surfactant. The final black colour precipitate was dried at room temperature for 24 h.

2.3 Catalytic Activity

2.3.1 Degradation of MB

a) Degradation of MB Using $NaBH_4$ in Presence of NiO Nanomaterials

In a degradation experiment, an aqueous solution of $NaBH_4$ (2 mL, 2×10^{-2} M) and MB (2 mL, 2×10^{-5} M) was mixed well, which acted as a control. To this solution, as-prepared NiO nanomaterials (2 mg) were added, and the solution was subjected to UV–Vis spectral analysis, and the absorption was recorded at regular intervals of time. As the time progressed, the decolorization of MB was observed, indicating the efficient performance of the catalyst.

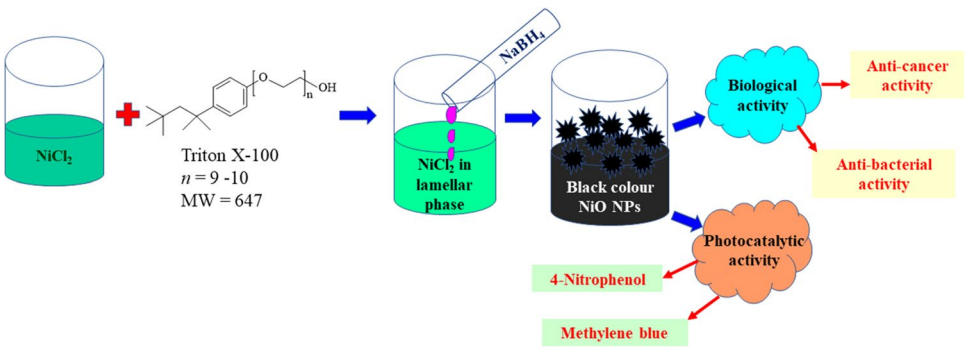

Scheme 1 Preparation of NiO nanomaterials in a lamellar LLC template

b) Degradation of MB Using Only $NaBH_4$

The degradation of MB was also carried out using only $NaBH_4$ in the absence of NiO nanomaterials. In this experiment, an aqueous solution of $NaBH_4$ (0.5×10^{-2} M) and MB (0.25×10^{-5} M) was mixed well, and the solution was subjected to UV–Vis spectral analysis. The absorption was recorded at regular intervals of time.

c) Degradation of MB Using Only NiO Nanomaterials

In this experiment, an aqueous solution of MB (0.25×10^{-5} M) and the NiO nanomaterials (80 mM, 300 µL) was mixed well. The solution was subjected to UV–Vis spectral analysis, and the absorption was recorded at regular intervals of time.

2.3.2 Reduction of 4-Nitrophenol

a) Reduction of 4-Nitrophenol Using $NaBH_4$ in the Presence of NiO

In a typical experiment, 4-nitrophenol (1 mM, 300 µL) was diluted with 5 mL of deionized water. After that, an ice-cold solution of $NaBH_4$ (0.1 M, 300 µL) was added and mixed well. To this mixture, as-prepared NiO nanomaterials (80 mM, 300 µL) were added. After adding NiO nanomaterials, the solution slowly decolorized from yellow to black. The solution was subjected to UV–Vis analysis, and the absorption was recorded at regular intervals of time.

b) Reduction of 4-Nitrophenol Using Only $NaBH_4$

In this experiment, an aqueous solution of 4-nitrophenol (0.25×10^{-3} M) and $NaBH_4$ (0.1 M) was mixed well. The solution was subjected to UV–Vis spectral analysis, and the absorption was recorded at regular intervals of time.

c) Reduction of 4-Nitrophenol Using NiO Nanomaterials

In this experiment, an aqueous solution of 4-nitrophenol (0.25×10^{-3} M) and NiO nanomaterials (80 mM, 300 µL) was mixed well. UV–Vis spectra of the solution was recorded at regular intervals of time.

2.4 Anti-Bacterial Activity of NiO Nanomaterials

The anti-bacterial activity of NiO nanomaterials was studied for gram-negative bacteria, *E. coli,* and gram-positive bacteria, *S. aureus,* through the well diffusion method. The test organism was swabbed with sterile cotton and inoculated on Muller-Hinton agar plates in wells of about 5 mm in diameter. The broth culture of both strains was used for the anti-bacterial assay. Three various concentrations of nanomaterials, namely 25, 50, and 100 µg/mL, were added to the petri plates, and the culture medium was incubated at 37 °C for 24 h. Afterwards, the zone of inhibition around the wells was measured using a ruler.

2.5 Anti-*Cancer* Activity of NiO Nanomaterials Towards MCF-7 Cells

The cytotoxic activity against MCF-7 (a breast cancer cell line) was tested using dimethyl thiazolyl tetrazolium bromide (MTT) assay [28]. In vitro, MCF-7 cell lines were plated in 96-well plates (1×10^5 cells/well) in dimethyl sulfoxide (DMSO) medium containing 10% foetal bovine serum (FBS). The MCF-7 cells were exposed to NiO nanomaterials at different concentrations (6.5, 12.25, 25, 50, and 100 µg/mL) and incubated for 24 h. Following NP exposure, 10 µL of MTT (5 µg/mL) was added and kept in a CO_2 incubator for 4 h. The supernatant was removed, and 100 µL of DMSO was added to each well.

3 Results and Discussion

The preparation of stable NiO nanomaterials in an LLC medium using a chemical reduction method is described. A mixture of water and TX-100 [3.2 mL: 6.8 mL; 0.8: 1.7 wt%] exhibited the LLC phase having a lamellar ordering at 4 °C. The LLC medium is known to offer a controlled reaction medium for the growth of nanomaterials, and the medium also acts as a stabilising agent for the formed particles by preventing their aggregation. In this present study, the preparation of NiO nanomaterials was carried out in the lamellar LLC medium using $NaBH_4$ as the reducing agent without using any external stabilising agent. The addition of a reducing agent caused a change in the colour of the $NiCl_2$ solution from green to black indicating the formation of nanomaterials.

3.1 UV- Visible and FT-IR Spectroscopy Analysis

A UV–Vis spectrum of NiO nanomaterials is shown in Fig. 1a**.** The commonly observed surface plasmon resonance (SPR) value for the NiO nanomaterials is ~ 374–422 nm [29]. The phenomenon of SPR is due to the coherent oscillation of conduction electrons as a result of the absorption of light. The UV–Vis spectrum of the dilute dispersion of NiO nanomaterials displayed a band at 341 nm, which indicated the formation of NiO nanomaterials. The band gap energy of the NiO nanomaterials was 4.6 eV, as calculated from the UV-DRS spectrum of the nanomaterials (Fig. S1).

A FT-IR spectrum recorded for NiO nanomaterials is shown in Fig. 1b. The spectrum exhibited the characteristic peaks at 454 cm^{-1}, 656 cm^{-1}, 1052 cm^{-1}, 1280 cm^{-1}, 1460 cm^{-1}, 1641 cm^{-1},2065 cm^{-1} and 3470 cm^{-1}. The bands at 454 and 656 cm^{-1} indicated the presence of NiO nanomaterials [30]. The carbonate groups, which result from the samples' reaction with CO_2 from the air during the analysis process, are responsible for the peaks observed at around

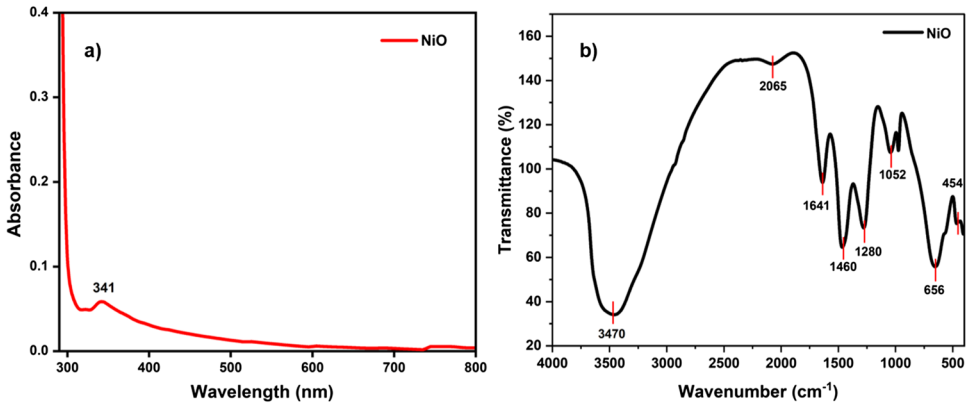

Fig. 1 (**a**) UV–Vis spectra (**b**) FT-IR spectrum of NiO nanomaterials

2065 cm^{-1}, 1460 cm^{-1}, 1280 cm^{-1} and 1052 cm^{-1} [30–32]. A broad peak at 3470 cm^{-1} is because of the stretching of O–H and the peak at 1641 cm^{-1} corresponds to bending vibrations, from the adsorbed water molecules. The FT-IR spectrum did not show the peaks corresponding to $NaBH_4$ thus confirming its removal [33].

3.2 Morphological Studies

The TEM images of the NiO nanomaterials with different magnifications are shown in Fig. 2. The TEM images displayed nanosheet-like morphology having an average lateral size of nearly 150–180 nm. However, close observation of the images revealed a folded layer structure. Likewise, the surface morphology of the nanomaterials was also investigated by SEM analysis. The SEM images of the prepared NiO nanomaterials at two different magnifications are given in Fig. S2, which displayed agglomerated network.

3.3 XPS Analysis

The purity and composition of the nanomaterial sample were studied by XPS measurements. An overall XPS survey spectrum of NiO is shown in Fig. 3a. The spectrum displayed five sharp peaks with varied intensities, which indicated the presence of C, O, and Ni. The C1s showed a single peak at 286.47 eV (Fig. 3b). The peak at 532.15 eV is due to O1s (Fig. 3c). The two sharp peaks obtained at binding energies of 856.97 eV and 874.63 eV (Fig. 3d) correspond to Ni $2p_{3/2}$ and Ni $2p_{1/2}$, while their satellite peaks due to the shake-up process appeared at 862.89 eV and 880.79 eV, respectively, which confirmed the presence of NiO nanomaterials [34]. The spin–orbit splitting between the Ni $2p_{3/2}$ and Ni $2p_{1/2}$ core levels of NiO nanomaterials is 17.66 eV.

3.4 Catalytic Activities of the NiO Nanomaterials and $NaBH_4$ for the Degradation of MB and Reduction of 4-Nitrophenol

The degradation of MB was investigated using NiO nanomaterials and $NaBH_4$ under visible light irradiation at room temperature. The UV–Vis spectrum of the aqueous solution of MB (2 mL, 2.3×10^{-5} M) showed an absorption peak at around 665 nm. Upon addition of NiO nanomaterials (300 µm) with $NaBH_4$, the intensity of the peak at 665 nm decreased gradually with time indicating the degradation of the dye. An overlap of absorption spectra at regular time interval of 2 min (from 0 to 22 min) is shown in Fig. 4a. The reduction follows pseudo-first-order kinetics with respect to MB. (Since $NaBH_4$ is excess compared to MB, its concentration will not change significantly] and rate is equal to $r = k\prime[\mathrm{MB}]$ where $k\prime = k[NaBH4]$. The rate constant was calculated from the slope of the graph and is found to be 0.5×10^{-2} min^{-1} (Fig. 4b).

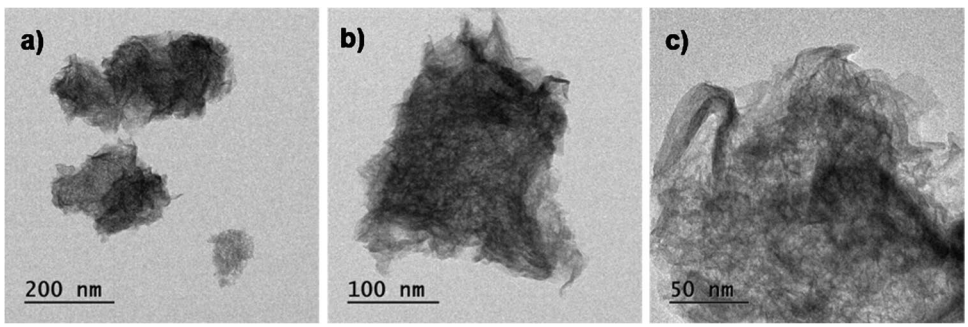

Fig. 2 TEM images of NiO nanomaterials at different magnification of (**a**) 200nm (**b**) 100nm and (**c**) 50nm

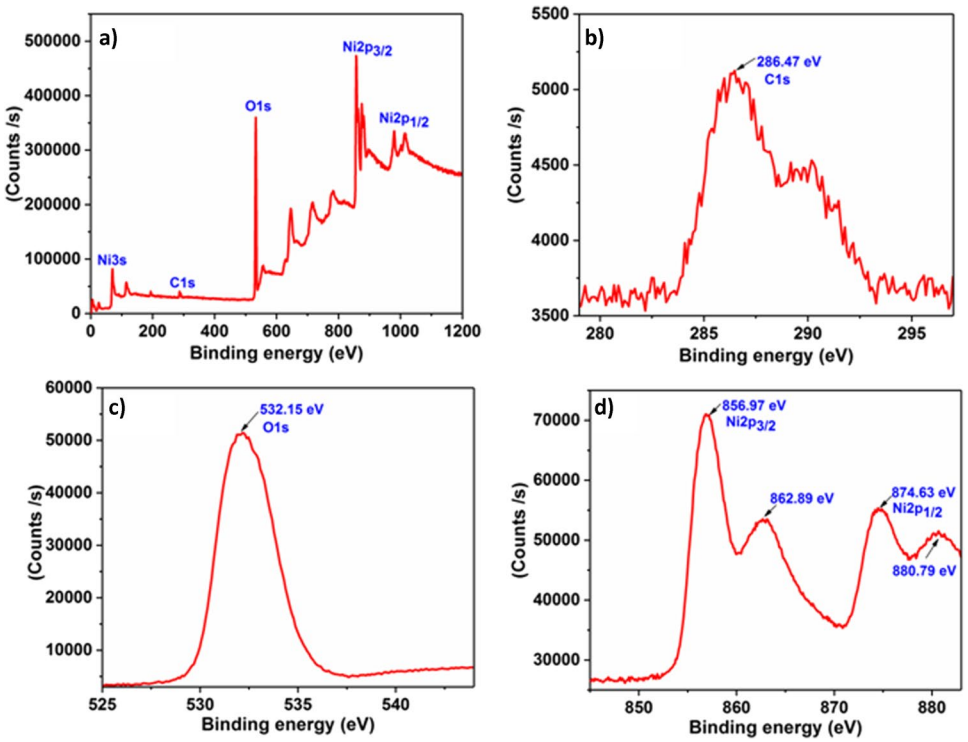

Fig. 3 XPS spectra for NiO nanomaterials **a**) survey spectrum **b**) C1s **c**) O1s **d**) Ni 2p core level spectrum

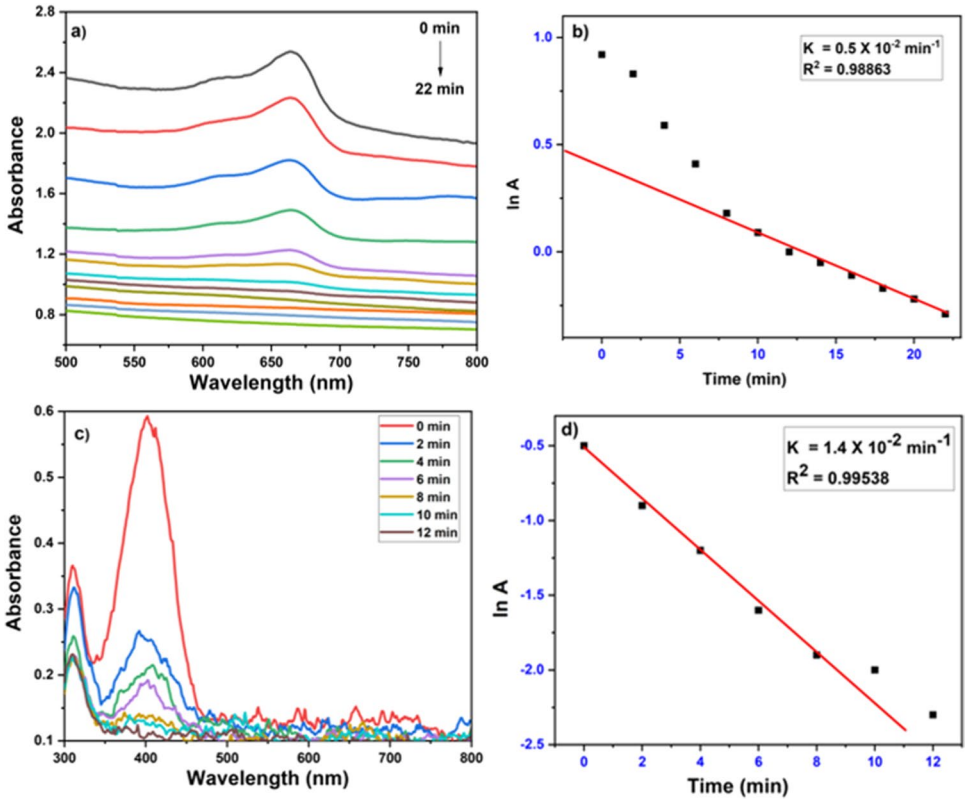

Fig. 4 UV–Vis absorption spectra for the degradation of **a**) MB and reduction of **c**) 4-nitrophenol using $NaBH_4$ in the presence of NiO nanomaterials at regular time interval of 2 min; **b** and **d** are corresponding plot of lnA *versus* time, respectively

There have been few reports on the catalytic application of NiO nanomaterials for the degradation of MB. It is interesting to point out here that Khairnar and Shrivastava synthesised NiO nanomaterials by a chemical route utilising $NiCl_2$ and $NaHCO_3$ as the precursors [30]. The resulting spherical-shaped NiO nanomaterials, having a size of 6.36 nm, were used for the photocatalytic degradation of MB in the presence of visible light irradiation. The kinetic investigation of the photocatalytic degradation of MB showed a rate constant value of 4.6×10^{-1} min^{-1}. Vidya and Balamurugan reported the degradation of MB using PANI-NiO nanocomposite under visible light irradiation [35]. The authors synthesised the nanocomposite via the oxidative polymerization method. The average length of the nanocomposite was in the range of 5–10 nm and showed nanofibrillar morphology with agglomeration. A rate constant of 4.7×10^{-3} min^{-1} was observed for the degradation of MB using the PANI-NiO nanocomposite.

Further, catalytic activity of NiO nanomaterials for the reduction of 4-nitrophenol using $NaBH_4$ was also investigated. For the experiment, $NaBH_4$ (0.1 M, 300 µL), 4-nitrophenol (1 mM, 300 µL), and NiO nanomaterials (80 mM, 300 µL) were used. An aqueous solution of 4-nitrophenol and $NaBH_4$ exhibited an absorption band with λ_{max} at 400 nm due to the 4-nitrophenolate anion. There was no change in the intensity of the peak in the absence of the catalyst. After the addition of the catalyst, the intensity of the band at 400 nm gradually decreased, accompanied by the appearance of a new band at 310 nm due to the formation of 4-aminophenol. The initial light-yellow colour of the 4-nitrophenol turned to an intense yellow with the addition of $NaBH_4$, and after the addition of the catalyst, the solution slowly decolourized from yellow to brown colour that darkened with time. The absorption spectra recorded at a regular interval of 2 min are shown in Fig. 4c. A plot of logarithm of the absorbance (lnA) *versus* reaction time is provided in Fig. 4d**,** which is a straight line. The apparent rate constant was calculated from the slope of this linear progression and found to be 1.4×10^{-2} min^{-1}.

Additionally, degradation of MB was studied using only $NaBH_4$ and NiO nanomaterials alone at room temperature. UV–Vis spectra for the reduction using only $NaBH_4$ at different intervals from 0 min to 18 h, is shown in Fig. S3a) and using only NiO nanomaterials is given in Fig. S3b). The spectral analysis showed that, for an observed period of 18 h, the degradation of MB with NiO was more pronounced compared to that of MB with $NaBH_4$. In both the cases, the characteristic peak at 665 nm decreased as the time increased. However, the peak did not disappear even after 18 h which suggest incomplete degradation of MB and perhaps a longer time period might result in complete degradation.

The reduction of 4-nitrophenol using $NaBH_4$ and NiO nanomaterials separately was also examined under UV–Vis spectroscopy. The spectra recorded at different intervals for the reaction mixture containing only $NaBH_4$ is given in Fig. S3c). Similarly, the spectra recorded using only NiO nanomaterials is shown in Fig. S3d). The reduction of 4-nitrophenol using NiO nanomaterials is efficient than the reduction of 4-nitrophenol using $NaBH_4$, as shown in Fig. S3c). All these experiments indicated that the degradation of MB and reduction of 4-nitrophenol completed efficiently in a shorter period while using both NiO nanomaterials and $NaBH_4$.

The reduction of 4-nitrophenol and the degradation of MB using only $NaBH_4$ and only NiO, the performance of NiO was better, however both processes took longer time compared to the reaction using both $NaBH_4$ and NiO together. Further, the reactions did not complete till the observed period of around 19–20 h. Moreover, for the reactions using only $NaBH_4$ and only NiO, readings recorded were not at regular intervals. The absorbance vs. wavelength graphs are provided in Fig. S3. The ln A vs. time graphs for the reactions using only $NaBH_4$ and only NiO are provided in Fig. S4. Therefore, a direct comparison of data in Fig. 4 where experiments were carried out at regular intervals of time and Fig. S4 where the readings were acquired at irregular intervals is not feasible.

The NiO nanomaterials (along with $NaBH_4$) also showed good recyclability up to four cycles, and particles can be collected and reused without significant loss in their catalytic activity (Fig. S5). However, the time required for the completion of the reduction increased with increasing cycles. Ramu and Choi reported the PdO-NiO nanocomposite via the hydrothermal combined calcination process [36]. The spherical PdO-NiO nanomaterials were evaluated for the catalytic activity for the reduction of 4-nitrophenol and degradation of MB in presence of $NaBH_4$. The nanocomposite exhibited a rate constant of 1.667×10^{-1} min^{-1} for 4-nitrophenol and 9.9×10^{-2} min^{-1} for MB dye.

3.5 Anti-Bacterial Activity of NiO Nanomaterials

The anti-bacterial activity of NiO nanomaterials was studied using the well diffusion method against *E. coli* and *S. aureus* bacteria. For different amounts of NiO nanomaterials (25, 50, and 100 µg/mL), the inhibition zones measured were 19, 20, and 22 mm for gram-positive (*S. aureus),* and the corresponding values for gram-negative (*E. coli*) were 13, 15, and 16 mm (Table 1). The anti-bacterial activity increased as the concentration of NiO nanomaterials increased. It can be clearly seen that the activity of NiO

Table 1 Zone of inhibition (mm) of NiO nanomaterials against bacterial strains tested

Concentration (µg / mL)	Zone of Inhibition (mm)	
	E. coli	*S. aureus*
25	19	13
50	20	15
100	22	16

nanomaterials against *S. aureus* was higher than that of *E. coli,* as shown in Fig. 5.

A few examples of biological applications of NiO nanomaterials reported in the literature are given below. Khashan et al. prepared the NiO NP by laser ablation of nickel metal in water [37]. The authors tested the anti-microbial activity using broth medium against *Pseudomonas aeruginosa*, *E. coli* (gram-negative), *S. aureus,* and *Streptococcus pneumonia* (gram-positive) bacteria. The Ni nanomaterials (1000 µg mL^{-1}) were effective bactericidal agents for both strains but more effective against gram-positive than -negative strains. Hussein and Mohammed prepared the NiO nanomaterials using an aqueous grape extract as reducing agents [38]. The authors studied the anti-bacterial activities of NiO nanomaterials against gram-positive (*S. aureus*) and gram-negative (*K. pneumoniae*) bacteria. In this study, the anti-bacterial effect increased as the concentration of NiO increased from 0.0025 M to 0.02 M. For a higher concentration of NiO (0.02 M), the zone of inhibition was 21 mm and 17.75 mm for *S. aureus* and *K. pneumoniae,* respectively. These studies indicated that NiO nanomaterials were more effective against gram-positive bacteria than gram-negative bacteria. A similar behaviour was observed in our present study as well.

The mechanism of bacterial killing includes the production of reactive oxygen species, cation release, biomolecule damages, ATP depletion, and membrane interaction. Three types of mechanisms have been proposed for the anti-bacterial activity of the NiO nanomaterials,

oxidative stress causing by reactive oxygen species (ROS) generated,
interaction of Ni^{2+} with proteins
the destruction of the bacteria cells via strong affinity interaction between Ni^{2+} and cell membrane

It was noticed that NiO nanomaterials triggers the oxidative stress, protein dysfunction, membrane and DNA damage, leading to microbial cell damage [39].

3.6 MTT Assay of In-Vitro MCF-7 Cells

The cytotoxic efficacy of NiO nanomaterials against breast cancer cell lines was studied by using MTT assay. Figure 6 shows the dose-dependent (6.5, 12.5, 25, 50, and 100 µg/mL) cytotoxic effect against in vitro MCF-7 cell lines. Following 24 h of incubation, there was significant cytotoxic activity against in vitro cells. The percentage of cytotoxic activity of NiO nanomaterials was observed as 12.25%, 18.97%, 36.36%, 43.87%, and 58.89% for MCF-7 cells, as shown in Graph 1**.** The cell incubation was increased with increasing concentrations of NiO nanomaterials. The results of the cytotoxic study matched the earlier reports [27, 40]. The half maximal inhibitory concentration (IC_{50} value) was observed as 78.93 µg/mL for NiO nanomaterials against breast cancer cell lines by MTT assay. This result revealed the good cytotoxic effect of NiO nanomaterials against MCF-7 breast cancer cells.

4 Comparative study

There are not many reports regarding the anti-cancer activity of NiO nanomaterials against MCF-7 cell lines. A few available reports are mentioned in Table 2. The study by Abbaszadeh et al. described the cytotoxic and anti-cancer activity of nickel oxide at glutamic and thiosemicarbazide NPs (NiO at Glu and TSC) against breast cancer cells and reported an IC_{50} value of 298.33 [27]. A similar study involving ZnO NPs reported an IC_{50} value of 121 [40]. The IC_{50} value of NiO nanomaterials in the present study, which is the concentration of nanomaterials that can cause the death of 50% of the cancer cells, is 78.93. The smaller IC_{50} value compared to the other reports [27, 40] indicates better anticancer activity of the prepared NiO nanomaterials.

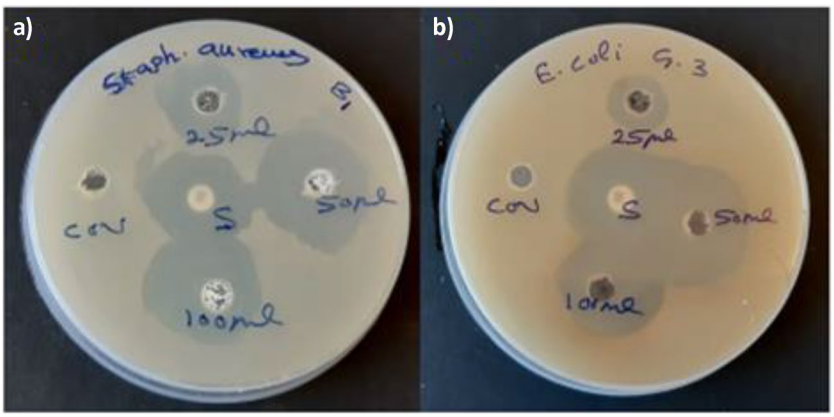

Fig. 5 Anti-bacterial activity of NiO nanoparticles against (**a**) *S. aureus* (**b**) *E. coli* (25 mL, 50 mL and 100 mL in (**a**) and (**b**) corresponds to 25 µg/mL, 50 µg/mL and 100 µg/mL)

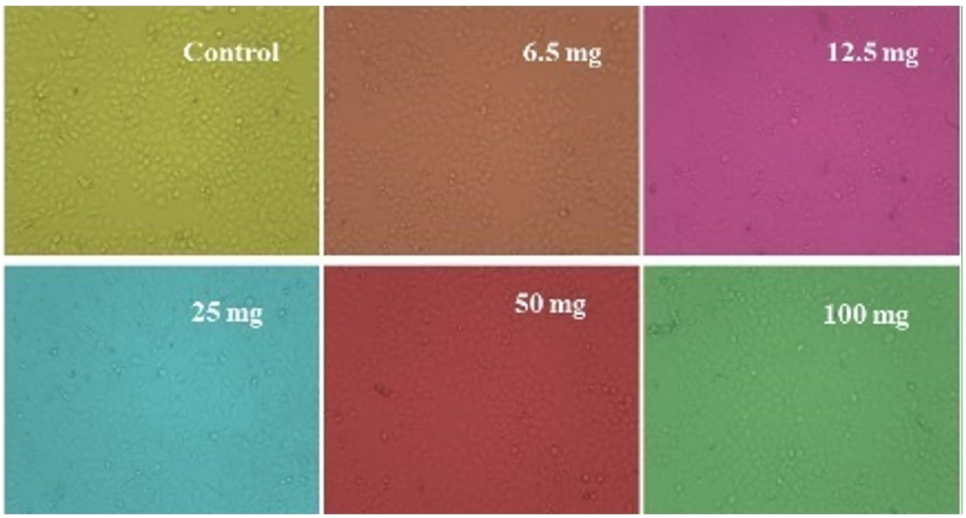

Fig. 6 Cytotoxicity assay of NiO nanomaterials against in-vitro MCF-7 cells for 24 h

Conc (µg/ml)	% Cell inhibition
6.5	12.25
12.5	18.97
25	36.36
50	43.87
100	58.89

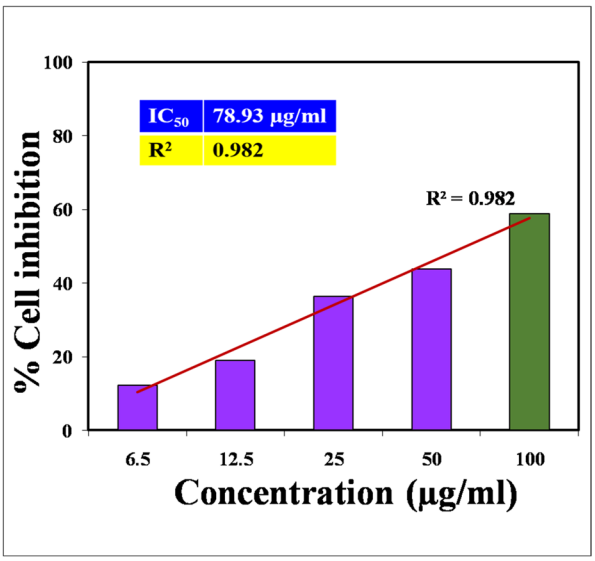

Graph 1 The graph displaying the % cell inhibition (against MCF-7 breast cancer cells) *versus* concentration of NiO nanomaterials soaked disks against

Table 2 A comparison of anti-cancer activity of the NiO nanomaterials for MCF-7 breast cancer cells with other reports

S. No	NPs	IC_{50}	Ref
1	NiO	78.93	Current study
2	NiO@Glu/TSC	298.33	27
3	ZnO	121	40

5 Conclusions

NiO nanomaterials were prepared in the lamellar medium by reducing the $NiCl_2.6H_2O$ using $NaBH_4$ at 4 °C. Sheet-like nanostructures having a lateral dimension of around 150–180 nm were observed in the TEM studies. The catalytic efficiency of the nanomaterials was evaluated for the reduction of 4-nitrophenol to 4- aminophenol and MB degradation. The rate constant values calculated for the degradation of MB and reduction of 4-nitrophenol were 0.5×10^{-2} min^{-1} and 1.4×10^{-2} min^{-1} respectively, using 2 mg and 80 mM of NiO nanomaterials respectively. The rate constant values are comparable to the other reported studies indicating the potential catalytic activity of the NiO nanomaterials. Further, anti-bacterial studies of the NiO nanomaterials against gram-positive (*S. aureus*) and gram-negative (*E. coli*) pathogens revealed that the nanomaterials were effective against gram-positive bacteria compared to gram-negative bacteria. Additionally, NiO nanomaterials showed a very good cytotoxic effect against the MCF-7 breast cancer cell line with an IC_{50} value of 78.93 µg/mL, which is lower compared to other literature reports indicating a good anti-cancer efficiency of prepared NiO nanomaterials.

Supplementary Information The online version contains supplementary material available at https://doi.org/10.1007/s12668-024-01572-0.

Acknowledgements S.U. acknowledges the Science and Engineering Research Board (SERB), Department of Science and Technology, New Delhi [Grant No. CRG/2020/003416] for funding thorough core research grant scheme. S.U. also thanks UGC-FRP scheme. Authors also thank MHRD-RUSA 2.0, Department of Education, New Delhi [Letter No. F.24/51, 2014-U] and Department of Science and Technology, New Delhi (No. SR/PURSE Phase 2/38(G), dt 29.12.2020) for the funding.

Author Contribution S.U. designed the work and supervised, PR.M., N.S., R.D., carried out experiment, analysis, and draft manuscript preparation. S.U. carried out draft corrections, all the others reviewed the manuscript.

Funding This study was funded by MHRD-RUSA 2.0, Department of Education, New Delhi [Letter No. F.24/51, 2014-U].

Data Availability No datasets were generated or analysed during the current study.

Declarations

The authors have no competing interests to declare that are relevant to the content of this article.

Ethical Approval Research do not involve human participants and / or animals.

Competing Interests The authors declare no competing interests.

References

1. Neto, A. M. F., & Salinas, S. R. A. (2005). *The physics of lyotropic liquid crystals: phase transitions and structural properties* (Vol. 62). OUP Oxford.
2. Guo, C., Wang, J., Cao, F., Lee, R. J., & Zhai, G. (2010). Lyotropic liquid crystal systems in drug delivery. *Drug Discovery Today, 15*(23–24), 1032–1040.
3. Wang, C., Chen, D., & Jiao, X. (2009). Lyotropic liquid crystal directed synthesis of nanostructured materials. *Science and Technology of Advanced Materials, 10*(20), 023001.
4. Dierking, I., & Al-Zangana, S. (2017). Lyotropic liquid crystal phases from anisotropic nanomaterials. *Nanomaterials, 7*(10), 305.
5. Qi, L., Gao, Y., & Ma, J. (1999). Synthesis of ribbons of silver nanoparticles in lamellar liquid crystals. *Colloids and Surfaces A: Physicochemical and Engineering Aspects, 157*(1–3), 285–294.
6. Patakfalvi, R., & Dékány, I. (2002). Preparation of silver nanoparticles in liquid crystalline systems. *Colloid and Polymer Science, 280*, 461–470.
7. Umadevi, S., Lee, H. C., Ganesh, V., Feng, X., & Hegmann, T. (2014). A versatile, one-pot synthesis of gold nanostars with long, well-defined thorns using a lyotropic liquid crystal template. *Liquid Crystals, 41*(3), 265–276.
8. Umadevi, S., Umamaheswari, R., & Ganesh, V. (2017). Lyotropic liquid crystal-assisted synthesis of micro-and nanoparticles of silver. *Liquid Crystals, 44*(9), 1409–1420.
9. Meyyathal, P. R., Santhiya, N., Umadevi, S., Michelraj, S., & Ganesh, V. (2019). Lyotropic liquid crystal directed synthesis of anisotropic copper microparticles and their application in catalysis. *Colloids and Surfaces A: Physicochemical and Engineering Aspects, 575*, 237–244.
10. Sheen Mers, S. V., Umadevi, S., & Ganesh, V. (2017). Controlled growth of gold nanostars: Effect of spike length on SERS signal enhancement. *ChemPhysChem, 18*(10), 1358–1369.
11. Narender, S. S., Varma, V. V. S., Srikar, C. S., Ruchitha, J., Varma, P. A., & Praveen, B. V. S. (2022). Nickel oxide nanoparticles: A brief review of their synthesis, characterization, and applications. *Chemical Engineering & Technology, 45*(3), 397–409.
12. Dharmaraj, N., Prabu, P., Nagarajan, S., Kim, C. H., Park, J. H., & Kim, H. Y. (2006). Synthesis of nickel oxide nanoparticles using nickel acetate and poly (vinyl acetate) precursor. *Materials Science and Engineering: B, 128*(1–3), 111–114.
13. Salavati-Niasari, M., Davar, F., & Fereshteh, Z. (2010). Synthesis of nickel and nickel oxide nanoparticles via heat-treatment of simple octanoate precursor. *Journal of alloys and Compounds, 494*(1–2), 410–414.
14. Gondal, M. A., Saleh, T. A., & Drmosh, Q. A. (2012). Synthesis of nickel oxide nanoparticles using pulsed laser ablation in liquids and their optical characterization. *Applied Surface Science, 258*(18), 6982–6986.
15. Danial, A. S., Saleh, M. M., Salih, S. A., & Awad, M. I. (2015). On the synthesis of nickel oxide nanoparticles by sol–gel technique and its electrocatalytic oxidation of glucose. *Journal of Power Sources, 293*, 101–108.
16. Sabouri, Z., Akbari, A., Hosseini, H. A., Khatami, M., & Darroudi, M. (2020). Egg white-mediated green synthesis of NiO nanoparticles and study of their cytotoxicity and photocatalytic activity. *Polyhedron, 178*, 114351.
17. Imran Din, M., & Rani, A. (2016). Recent advances in the synthesis and stabilization of nickel and nickel oxide nanoparticles: a green adeptness. *International journal of analytical chemistry, 2016*(1), 3512145.
18. Sabouri, Z., Akbari, A., Hosseini, H. A., Hashemzadeh, A., & Darroudi, M. (2019). Eco-Friendly Biosynthesis of Nickel Oxide Nanoparticles Mediated by Okra Plant Extract and Investigation of Their Photocatalytic, Magnetic, Cytotoxicity, and Antibacterial Properties. *Journal of Cluster Science, 30*(6), 1425–1434. https://doi.org/10.1007/s10876-019-01584-x
19. Sabouri, Z., Fereydouni, N., Akbari, A., Hosseini, H. A., Hashemzadeh, A., Amiri, M. S., & Darroudi, M. (2020). Plant-based synthesis of NiO nanoparticles using salvia macrosiphon Boiss extract and examination of their water treatment. *Rare Metals, 39*(10), 1134–1144. https://doi.org/10.1007/s12598-019-01333-z
20. Sabouri, Z., Akbari, A., Hosseini, H. A., Khatami, M., & Darroudi, M. (2020). Tragacanth-mediate synthesis of NiO nanosheets for cytotoxicity and photocatalytic degradation of organic dyes. *Bioprocess and Biosystems Engineering, 43*(7), 1209–1218. https://doi.org/10.1007/s00449-020-02315-7
21. Ghazal, S., Akbari, A., Hosseini, H. A., Sabouri, Z., Forouzanfar, F., Khatami, M., & Darroudi, M. (2020). Sol-gel biosynthesis of nickel oxide nanoparticles using Cydonia oblonga extract and evaluation of their cytotoxicity and photocatalytic activities. *Journal of Molecular Structure, 1217*, 128378. https://doi.org/10.1016/j.molstruc.2020.128378
22. Sabouri, Z., Akbari, A., Hosseini, H. A., Khatami, M., & Darroudi, M. (2021). Green-based bio-synthesis of nickel oxide nanoparticles in Arabic gum and examination of their cytotoxicity, photocatalytic and antibacterial effects. *Green Chemistry Letters and Reviews, 14*(2), 402–412. https://doi.org/10.1080/17518253.2021.1923824
23. Sabouri, Z., Rangrazi, A., Amiri, M. S., Khatami, M., & Darroudi, M. (2021). Green synthesis of nickel oxide nanoparticles using Salvia hispanica L. (chia) seeds extract and studies of their photocatalytic activity and cytotoxicity effects. *Bioprocess and*

Biosystems Engineering, 44(11), 2407–2415. https://doi.org/10.1007/s00449-021-02613-8
24. Prabhu, S., Thangadurai, T. D., Bharathy, P. V., & Kalugasalam, P. (2022). Synthesis and characterization of nickel oxide nanoparticles using Clitoria ternatea flower extract: Photocatalytic dye degradation under sunlight and antibacterial activity applications. *Results in Chemistry, 4*, 100285.
25. Ali, T., Warsi, M. F., Zulfiqar, S., Sami, A., Ullah, S., Rasheed, A., … Baig, M. M. (2022). Green nickel/nickel oxide nanoparticles for prospective antibacterial and environmental remediation applications. *Ceramics International*, *48*(6), 8331–8340.
26. Sahila, S., Prabhu, N., Simiyon, G. G., & Jayakumari, L. S. (2022). A novel green and eco-friendly synthesis of nickel oxide nanoparticles by auto combustion technique using Allium cepa bulb extract and their dielectric behaviour. *Chemical Data Collections, 38*, 100837.
27. Abbaszadeh, N., Jaahbin, N., Pouraei, A., Mehraban, F., Hedayati, M., Majlesi, A., … Salehzadeh, A. (2020). Preparation of novel nickel oxide@ glutamic/thiosemicarbazide nanoparticles: Implications for cytotoxic and anti-cancer studies in MCF-7 breast cancer cells. *Journal of Cluster Science*, 1–9.
28. Khalil, A. T., Ovais, M., Ullah, I., Ali, M., Shinwari, Z. K., & Maaza, M. (2020). Physical properties, biological applications and biocompatibility studies on biosynthesized single phase cobalt oxide (Co3O4) nanoparticles via Sageretia thea (Osbeck.). *Arabian Journal of Chemistry, 13*(1), 606–619.
29. Nouneh, K., Oyama, M., Diaz, R., Abd-Lefdil, M., Kityk, I. V., & Bousmina, M. (2011). Nanoscale synthesis and optical features of metallic nickel nanoparticles by wet chemical approaches. *Journal of Alloys and Compounds, 509*(19), 5882–5886.
30. Khairnar, S. D., & Shrivastava, V. S. (2019). Facile synthesis of nickel oxide nanoparticles for the degradation of Methylene blue and Rhodamine B dye: A comparative study. *Journal of Taibah University for Science, 13*(1), 1108–1118.
31. Sharma, A. K., Desnavi, S., Dixit, C., Varshney, U., & Sharma, A. (2015). Extraction of nickel nanoparticles from electroplating waste and their application in production of bio-diesel from biowaste. *International Journal of Chemical Engineering and Applications, 6*(3), 156.
32. Ghalmi, Y., Habelhames, F., Sayah, A., Bahloul, A., Nessark, B., Shalabi, M., & Nunzi, J. M. (2019). Capacitance performance of NiO thin films synthesized by direct and pulse potentiostatic methods. *Ionics, 25*, 6025–6033.
33. Ar, I., Guler, O. U., & Guru, M. (2018). Synthesis and characterization of sodium borohydride and a novel catalyst for its dehydrogenation. *International Journal of Hydrogen Energy, 43*(44), 20214–20233.
34. Mansour, A. N. (1994). Characterization of NiO by XPS. *Surface Science Spectra, 3*(3), 231–238.
35 Vidya, J., & Balamurugan, P. (2019). Photocatalytic degradation of methylene blue using PANi—NiO nanocomposite under visible light irradiation. *Materials Research Express, 6*(9), 0950c8.
36. Ramu, A. G., & Choi, D. (2021). Highly efficient and simultaneous catalytic reduction of multiple toxic dyes and nitrophenols waste water using highly active bimetallic PdO–NiO nanocomposite. *Scientific Reports, 11*(1), 22699.
37. Khashan, K. S., Sulaiman, G. M., Hamad, A. H., Abdulameer, F. A., & Hadi, A. (2017). Generation of NiO nanoparticles via pulsed laser ablation in deionised water and their antibacterial activity. *Applied Physics A, 123*, 1–10.
38. Hussein, B. Y., & Mohammed, A. M. (2021). Biosynthesis and characterization of nickel oxide nanoparticles by using aqueous grape extract and evaluation of their biological applications. *Results in Chemistry, 3*, 100142.
39. Zhang, Q., Lyu, Y., Huang, J., Zhang, X., Yu, N., Wen, Z., & Chen, S. (2020). Antibacterial activity and mechanism of sanguinarine against Providencia rettgeri in vitro. *PeerJ, 8*, e9543.
40. Boroumand Moghaddam, A., Moniri, M., Azizi, S., Abdul Rahim, R., Bin Ariff, A., Navaderi, M., & Mohamad, R. (2017). Eco-friendly formulated zinc oxide nanoparticles: Induction of cell cycle arrest and apoptosis in the MCF-7 cancer cell line. *Genes, 8*(10), 281.